ARTICLE

BIOTECHNOLOGY and BIOENGINEERING

A Novel System for Evaluation of Drug Mixtures for Potential Efficacy in Treating Multidrug Resistant Cancers

Daniel A. Tatosian,[1] Michael L. Shuler[1,2]

[1]School of Chemical and Biomolecular Engineering, Cornell University, New York

[2]Department of Biomedical Engineering, Cornell University, 115 Weill Hall, Ithaca, New York 14853; telephone: 607-255-7577; fax: 607-255-7330; e-mail: mls50@cornell.edu

Received 3 August 2008; revision received 17 November 2008; accepted 1 December 2008

Published online 5 December 2008 in Wiley InterScience (www.interscience.wiley.com). DOI 10.1002/bit.22219

ABSTRACT: Multidrug resistant (MDR) cancer is difficult to treat. Chemicals that are effective MDR modulators have never exited clinical trials as FDA approved products due to side effects. It has been hypothesized that using a combination of chemotherapeutics with a mixture of MDR modulators (each with different side effects) may lead to useful treatment strategies. Because the experimental space for combination treatments can be large, this space may be impracticable to explore using animal studies. Here we describe an in vitro system based on microfabrication and cell culture that can potentially be used to explore large experimental spaces efficiently. The Microscale Cell Culture Analog (μCCA) concept mimics the body's response using interconnected compartments that represent various tissues or organs. A μCCA is based on the structure of an appropriate physiologically based pharmacokinetic (PBPK) model and emulates the body's dynamic response to exposure to various drugs and chemicals. For this problem we have chosen a μCCA with living cells representing the liver (HepG2/C3A), bone marrow (MEG-01), uterine cancer (MES-SA), and a MDR variant of uterine cancer (MES-SA/DX-5). In proof of concept experiments we found in 24 h "acute" exposures and 72 h treatments that the μCCA system predicts combining the chemotherapeutic, doxorubicin, with cyclosporine and nicardipine, as MDR modulators will have greater efficacy than using doxorubicin by itself or with either modulator alone. This combined strategy is selective in inhibiting MES-SA/DX-5 cell proliferation and may prove to be advantageous in vivo by specifically targeting MDR cancer with acceptable side-effects. This cell specific synergy was not observed in traditional 96-well plate assays. By combining the μCCA with a PBPK model, appropriate drug doses and area under the curve exposure for in vivo trials can be extrapolated directly from the results obtained with this device. This device and approach should be useful in screening potential drug/modulator combinations to determine candidate treatments for MDR cancer. Indeed this approach may be useful for in vitro evaluation of human response to a wide range of exposures to mixtures of chemicals or drugs.

Biotechnol. Bioeng. 2009;103: 187–198.

KEYWORDS: cell culture analog; biological microdevices; physiologically based pharmacokinetics; microfluidics; multidrug resistant cancer

Correspondence to: M.L. Shuler

Contract grant sponsor: New York State Office of Science, Technology and Academic Research (NYSTAR) Program

Contract grant sponsor: National Science Foundation

Contract grant numbers: BES 0342985; ECS-9876771; ECS-9731293

Contract grant sponsor: Cornell Nano-Scale Science & Technology Facility

Additional Supporting Information may be found in the online version of this article.

Introduction

Several biological barriers limit the ability of physicians to treat cancer patients effectively. One such barrier is the ability of cancer cells in the body to develop cellular resistance to chemotherapy. Termed multidrug resistance (MDR), this cellular phenotype provides protection to the cell by preventing cytotoxic drugs from accumulating in the cytoplasm. It frequently occurs after treatment in patients who undergo relapse, but is also found in some cancers prior to any treatment (Johnstone et al., 1999).

The best-characterized mechanism of MDR in humans is over expression of the membrane transporter, P-glycoprotein (P-gp). Chemical modulators have been discovered that can functionally inhibit the action of this protein, and in vitro studies have shown a complete reversal of resistance (Borowski et al., 2005; Krishna and Mayer, 2000; Tsuruo et al., 2003). However, all modulators have failed in the clinical setting due to excessive toxicity arising from either the large concentrations of modulators required, or pharmacokinetic interactions with the combined chemotherapeutic.

Lehnert et al. (1991) and Pascaud et al. (1998) have speculated that a combination of modulator and chemotherapeutic(s) could be effective in treating MDR cancer

with minimal side effects. However, the potential experimental space expands greatly when multiple combinations of drugs in varying doses are to be tested. Indeed the experimental space could grow to be so large that animal studies would be impractical. An in vitro system, that captured some of the key pharmacokinetic interactions in the body, could explore a large experimental space to find a subspace where animal or clinical trials would most likely be successful.

In this article, we describe a novel system, termed a Microscale Cell Culture Analog or μCCA, to predict which combinations of these compounds are practical candidates. Typical in vitro methods only screen for efficacy, and neglect any interactions that might occur in the body. The μCCA device is designed to mimic key aspects of the pharmacokinetics of drug or toxin exposure in the body (Ghanem and Shuler, 2000; Shuler et al., 1996; Sin et al., 2004; Sweeney et al., 1995; Viravaidya and Shuler, 2004; Viravaidya et al., 2004). A μCCA is a microfabricated device containing several organ or tissue chambers connected together by microfluidic channels. Cell types representative of target and interacting tissues from the body are grown in corresponding "tissue chambers," with a recirculating blood surrogate (culture medium) flowing through the microchannels and carrying nutrients and metabolites from "tissue" to "tissue."

The scaling of all tissue sizes and blood surrogate perfusion rates is based on human parameters, producing physiologically realistic exposure and distribution patterns. The "tissues" are represented by cell lines that express a desired feature of the tissue. A limitation of this approach is that these cell lines cannot replicate the full range of activities and architecture of an in vivo tissue, but for well posed questions, such as in these proof-of-concept studies, cell lines that perform key, specific functions are sufficient. The device described in this article could, in principle, use three dimensional tissue engineered constructs or tissue slices to improve authenticity for a more complete representation of responses.

The interconnection between in vitro cell types in this flow device allows assessment of pharmacokinetic interactions. By using human cells the system may be more accurate than a rodent model. For example, the isoforms of P-gp expressed in rats differ significantly from humans (Hooiveld et al., 2002). A mathematical model that simulates adsorption, distribution, metabolism, and elimination (ADME) properties, such as a physiologically based pharmacokinetic model (PBPK), can be used to help understand and relate pharmacokinetic predictions made with the μCCA system to in vivo conditions. A PBPK simulates the body as a system of tissue "compartments" linked together in the same manner as blood flows through the circulatory system (D'Souza and Boxenbaum, 1988; Gerlowski and Jain, 1983).

Previously the potential usefulness of the μCCA concept was tested using naphthalene as a model toxicant. The system demonstrated that the hypothesis that naphthalene was converted into a reactive metabolite in the "liver" and could cause cell death in the "lung" compartment was plausible (Sin et al., 2004; Viravaidya et al., 2004). Further, 1,2-naphthalenediol and 1,2-naphthoquinone were shown to be the reactive metabolites responsible for cell death and that the presence of a "fat" compartment would modulate the severity of the response (Viravaidya and Shuler, 2004).

In this article we describe a μCCA specifically designed to test a combination of drugs for their ability to selectively attack MDR cancer without significant changes in side-effects. Further, we demonstrate how such experiments coupled with a PBPK can be used to relate these results to measurable human dose exposures.

Materials and Methods

Device Design and Fabrication

The μCCA device (Fig. 1a and b) was designed to fit on a 3 mm × 3 mm chip. Cell chamber sizes were scaled from human tissue data, and the corresponding culture medium perfusion rates were scaled to match organ residence times. The ratios of cell to total organ volume were used in the scaling calculations to account for the difference between the ideal ratio 2:1 cell to liquid, and the 1:5 value as a result of the chamber height. Organ and corresponding chamber parameters, and experimentally determined flow rates are listed in Supplementary Table I. The "other tissue" compartment is not on the silicon chip, but in a separate reservoir that also acts as a debubbler to vent gas bubbles and is necessary to capture the dynamic response in the body. The rest of the system is fabricated in silicon using traditional photolithographic and deep reactive ion etching techniques (Sin et al., 2004; Viravaidya and Shuler, 2004; Viravaidya et al., 2004). The chip housing was fabricated out of plexiglass as described previously (Sin et al., 2004). A 0.9 mm recess was machined into the plastic to accommodate the silicon chip and a 0.5 mm silicone pad (Grace-Bio Labs, Bend, OR), so that during assembly, the silicon chip is pressed firmly against the top plexiglass piece. Four screw holes were drilled to secure the enclosure (Fig. 1a). In the section "PBPK Simulation Equations and Parameters" the schematic structure of the PBPK diagrams for the human body and the μCCA device plus debubbler/reservoir are described.

Cell Culture

The four functional tissues in the device were represented by the following cell lines: HepG2/C3A (liver), MEG-01 (megakaryoblast, bone marrow), MES-SA (normal cancerous tissue), and MES-SA/DX-5 (multidrug resistant cancer tissue). All cells were obtained from the American Type Culture Collection. HepG2/C3A cells were cultured in MEM, MEG-01 cells in RPMI, and both MES-SA and MES-SA/DX-5 cells in McCoy's 5A medium. All media were

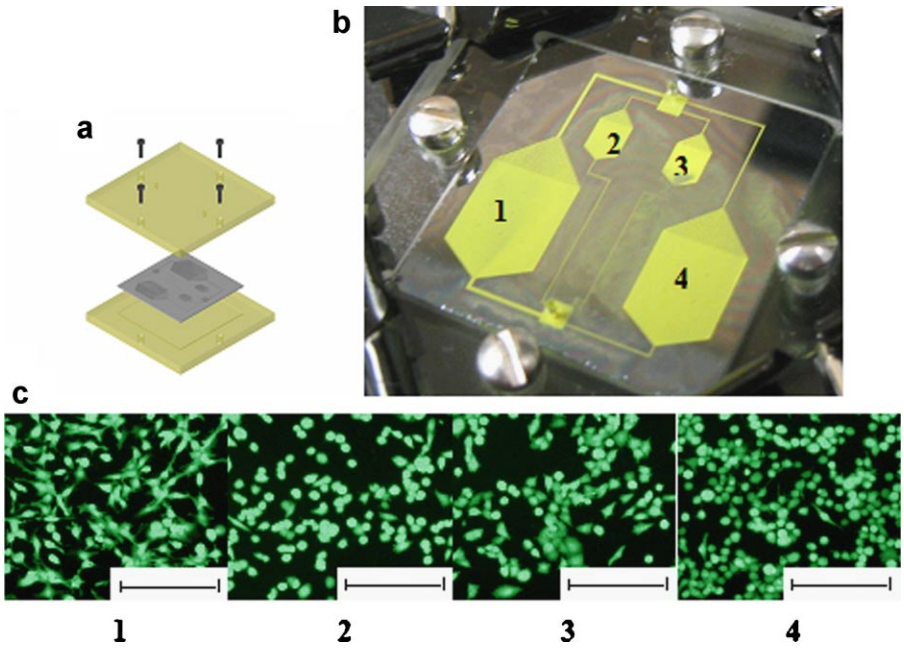

Figure 1. The μCCA device and representative images of cells growing on the chip. **a**: assembly drawing of device with the plexiglass chip housing. **b**: An image of the assembled device, which has been filled with a yellow dye as a contrast agent. **c**: Representative images of CellTracker Green labeled cells grown on the chip after 24 h of recirculating flow of control media. Cell types: (1) hepatocytes (C3A), (2) MDR cancer (DX5), (3) wild type cancer (MESSA), (4) megakaryocytes (MEG01). Scalebar shown is 200 μm. [Color figure can be seen in the online version of this article, available at www.interscience.wiley.com.]

supplemented with 10% FBS, unless otherwise noted. HepG2/C3A, MES-SA, and MES-SA/DX-5 were fed on the 3rd day, and passed on 6–7 days schedule using trypsin/EDTA. MEG-01 were passed every 3 days by scraping the bottom of the flask to resuspend the attached cells and diluted into two flasks at a ratio of 1:3. Cells were used up until 20 passages after receipt from ATCC, and stored in a mammalian culture incubator maintained at 37°C, 5% CO_2, and 95% humidity.

Cell Culture Analog Device Preparation and Operation

A 1 mm thick sheet of clear cell culture silicone (Grace Biolabs) was cut to fit over the silicon chips. Rectangular holes were cut out of this silicone sheet (termed "gasket") to match the culture chambers in the μCCA chip. When this silicone gasket is attached to the chip, these holes form a well above the culture chambers to aid in cell seeding. Both the μCCA chips and silicone pieces were cleaned by soaking in a mixture of 70% sulfuric acid and 10% hydrogen peroxide in water for 10 min. They were then rinsed in double distilled water, then placed together with the holes in the silicone sheet aligned to the culture chambers. The two pieces were then dried in a 70°C oven to allow the silicone to adhere to the chip surface. Then the chip-silicone pieces were autoclaved, and cooled prior to culturing.

The culture chambers were coated with 0.025 mg/mL poly-D-lysine (Sigma-Aldrich, St. Louis, MO) for 30 min, removed, and then coated with 0.05 mg/mL human blood plasma fibronectin (Chemicon International, Billerica, MA) for 30 min. The fibronectin solution was removed, and then each cell suspension was placed in the corresponding chambers to yield ~30% confluency using the following cell densities (cells/mm^2):

C3A : 620 MESSA : 900 DX5 : 900 MEG01 : 1600

This low confluency was chosen to simplify image analysis of viable cells for short-term experiments, and to permit room for growth during 3 day experiments. The chips were then incubated for 4 h to allow complete attachment, then flooded with McCoys5A medium containing 10% FBS and incubated until assembly.

Before assembly, the chip housings were cleaned in 70% alcohol, and then sterilized in an oxygen plasma cleaner (Harrick Plasma, Ithaca, NY). The cultured μCCA chips were then inserted into the chip housings and sealed. Recirculating flow is provided by a peristaltic pump (Watson-Marlow Bredel Inc., Wilmington, MA) with Pharmed tubing (Cole-Parmer, Vernon Hill, IL) connecting the chip inlet and outlet to an external reservoir which represents the "other tissues" compartment. This reservoir is made from a well from a 96-well plate, and is used to trap bubbles that are generated by the pump, to serve as a surge

tank, and as a sample port for medium sampling. The blood surrogate used is cell culture medium (McCoys 5A) supplemented with 10% FBS. The entire system is placed inside of the mammalian cell incubator, and operated at a flow rate of 3.6 μL/min.

Cell Culture Analog Device Assays

Three assays were used to generate the results presented. These assays utilize fluorescence measurements captured with a fluorescent microscope and camera after exposure to test compounds in the recirculating blood surrogate. Cell proliferation in the device was assayed with the long-term cell label CellTracker Green (Invitrogen Corp., Carlsbad, CA). Cells were incubated on-chip prior to assembly with 10 μM CellTracker Green in McCoys 5A without serum for 45 min at room temperature. By capturing images with a FITC filter cube (Ex:Em 465/530), we can visualize what level of confluency is reached during the drug study. Two controls are used for these experiments. The first is a no-flow control, and consists of cells cultured on μCCA chips, but incubated in a petri dish with culture medium instead of in the enclosed plexiglass housings. The second control is an assembled μCCA device with blood surrogate containing no test compounds. The two controls are needed to insure that the response is due to the drugs added and not due to the device itself or its operation.

For viability studies, an intracellular assay for viability was developed combining CellTracker Green and the live cell stain Celltrace Blue AM (Invitrogen). CellTracker Green labeling was performed as described for the proliferation assay. After incubation of the device with the recirculating test compounds, Celltrace Blue was recirculated through the device at ~6 μL/min for 75 min. By imaging with both a UV (Celltrace Blue) and a FITC (CellTracker Green) filter cube, viable and apoptotic/dead cells can be discriminated by direct comparison of both images. Viable cells are labeled strongly with both CellTracker Green and Celltrace Blue, while compromised cells are labeled by CellTracker Green with faint or negligible Celltrace Blue labeling. This labeling method is compared with SYTOX green, a common dead cell stain, in Supplementary Figure 1.

To facilitate assessment of relative drug accumulation, we chose to use an autofluorescent chemotherapeutic, doxorubicin, as the test compound. This chemical emits orange red fluorescence upon exposure to blue-green light. A TRITC filter cube (Ex:Em 530/595) was used in the collection of these images, and then images were processed to determine uptake in terms of relative fluorescence. This assay is performed in conjunction with either a 3-day cell proliferation assay or a 1-day cell cytotoxicity assay.

The drug doxorubicin is known to intercalate into DNA inside of the cell nucleus, and this binding amplifies the molar fluorescence intensity (Gigli et al., 1988; Karukstis et al., 1998; Kirchmeier et al., 2001). Therefore for image analysis, the brightest pixel in each cell is considered to represent the DNA bound drug. This value for each cell is averaged over all counted cells to determine the average relative drug bound to the cell.

Image Analysis

Image analysis in all cases was performed using ImagePro Plus software (Media Cybernetics, Bethesda, MD). Images were analyzed by using the count/size feature in ImagePro Plus to select each independent cell or cell clump based on threshold values.

Statistical Analysis

μCCA experimental data were analyzed using a general linear model (GLM) in Minitab (Minitab, Inc., State College, PA). Both μCCA experimental sets—short-term and long-term—were performed with an incomplete block design, due to limitation of number of concurrent samples. GLM's were formed with treatment as the independent variable, and the block (week) and chip-to-chip variation were accounted for as random effects. Each cell chamber was imaged in four consistent locations (center of each quarter section), although missing data did occur due to bubbles or other sample defects. Each cell type was analyzed separately, with a minimum of n (chips) = 40 for a given cell type, and minimum images analyzed of 140, spread among five treatments. Each data set was tested for normality by inspection of normal probability plots and histograms of residuals generated with the GLM, and accuracy of model was inspected by examining plots of residuals versus fitted values and versus order of data. Comparisons within a sample set to determine significance were performed with Tukey's pairwise comparison, $\alpha = 0.05$. Error bars on all μCCA figures represent the standard error from the GLM.

MTS Assays

The Celltiter 96 MTS reagent (Promega, Madison, WI) was used to determine viable cell density in a 96-well plate format, following standard protocols from the manufacturer. Briefly, cultures were incubated in 96 well plates for 1–3 days with 100 μL of drug mixture, in serial dilutions to facilitate the generation of dose–response curves. Following drug incubation the wells were rinsed with DPBS, then incubated with 100 μL fresh media and 20 μL MTS reagent for 1–4 h at 37°C (Wong et al., 2001). Results were determined on a platereader at 490 nm wavelength. EC values were determined by interpolation of the dose–response curves.

Estimation of DOX Metabolism by C3A Cells

DOX is metabolized into several metabolites, one of which is doxorubicinol (DOXOL). This metabolite is known to be <10% as potent as DOX at inhibiting tumor cell growth, but

is known to have other toxic properties to the body such as cardiotoxicity (Olson et al., 1988). It has also been shown to be 10% as cytotoxic as DOX to bone marrow blood progenitors such as granulocytic–monocytic colony-forming units (Dessypris et al., 1986). To approximate DOX metabolism, C3A cells were grown in T25 flasks and exposed to different concentrations of DOX in MEM/10% FBS. Samples of 50 μL were removed from the flask at specified time points (multiple flasks were used) and frozen down. To process the samples, we directly followed the protein precipitation step and a similar HPLC analysis to Zhou and Chowbay (2002). Peak area was measured and calibrated with DOX standards. We were not able to obtain DOXOL standards, so the concentrations were estimated by scaling the calibration for DOX by the molar fluorescence ratio of 1.7 (ratio of DOXOL:DOX; Zhou and Chowbay, 2002). The concentration versus time data (Fig. 2) was found to fit reasonably well to a set of first order metabolism equations:

$$\begin{aligned} V\frac{\mathrm{d}}{\mathrm{d}t}C_{\mathrm{DOX}} &= -(k_1 + k_{\mathrm{E}})\mathrm{ANC}_{\mathrm{DOX}} \\ V\frac{\mathrm{d}}{\mathrm{d}t}C_{\mathrm{DOXOL}} &= k_1\mathrm{ANC}_{\mathrm{DOX}} \end{aligned} \quad (1)$$

where V is the volume, C the concentration, k the reaction constant (1 for conversion to DOXOL, E for other net elimination), N the cell number. This does not take into account further metabolism of DOXOL, although additional metabolites were detected. The concentration of these metabolites was too small to accurately determine.

Estimation of Equilibrium Partition Coefficient in Cell Lines

Cells were suspended at a concentration of 2.5×10^6 cells/mL and incubated with 5 or 10 μM DOX in a 15 mL tube for 1 h on a rocker plate. Four 1.2 mL samples were removed for cellular extraction (following an adaption of the method of Anderson et al. (2002)). The medium from the first spin was also collected, and 50 μL processed using the method of Zhou and Chowbay (2002). Fluorescent HPLC detection was used to quantify the amount of DOX and DOXOL (and other metabolites) present in the cells and culture medium (following the protocol and mobile phase of Zhou and Chowbay (2002). Partition coefficients were calculated as cell concentration per free medium concentration.

Estimation of Plasma-Compartment Partition Coefficient

The plasma-compartment partition coefficient for the human model is obtained by converting the bound fraction value of 0.74 (Maniez-Devos et al., 1985):

$$\mathrm{partition} = \frac{1}{\mathrm{free}} - 1 \quad (2)$$

To calculate the μCCA plasma-compartment partition, we assume a linear binding relationship for protein binding. Maniez-Devos et al. (1985) have found that the majority of DOX in the blood is bound to albumin:

$$\mathrm{free} = \frac{1}{1 + kC_{\mathrm{Albumin}}} \quad (3)$$

Blood typically contains 34–54 mg/mL albumin, while Gibco FBS contains 30–50 mg/mL. We use 10% FBS in the cell culture medium, which results in an ~10-fold lower partition coefficient for the plasma compartment.

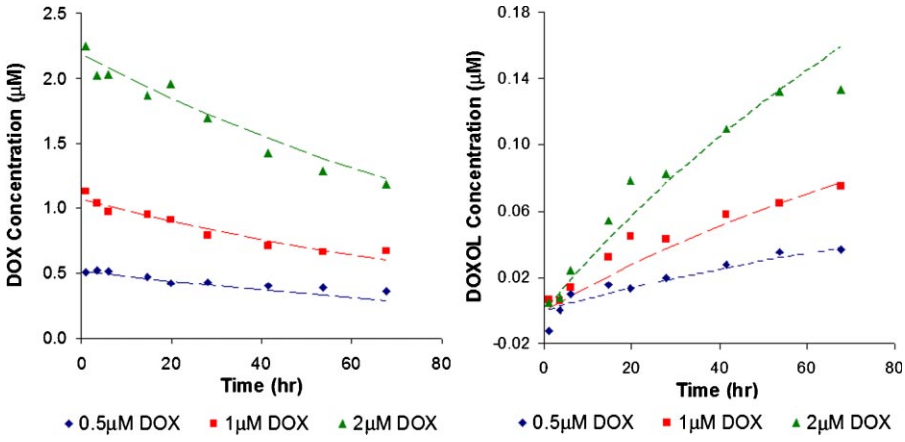

Figure 2. Measured DOX and DOXOL in culture medium during incubation with C3A cells in MEM w/10% FBS. Dashed lines are curve fits to the data. Each data point is the average of two separate medium samples that were processed individually (extraction, HPLC run). Fit values: $k_1 = 1.28\mathrm{E}{-9}$ cm^3/(h cell), $k_{\mathrm{E}} = 7.73\mathrm{E}{-9}$ cm^3/(h cell). [Color figure can be seen in the online version of this article, available at www.interscience.wiley.com.]

PBPK Simulation Equations and Parameters

The simple flow-limited case was assumed for this PBPK model. The basic equations solved are:

$$\begin{aligned} V\frac{\mathrm{d}}{\mathrm{d}t}C_i &= F\left(\frac{C_\mathrm{p}}{R_\mathrm{p}}-\frac{C_i}{R_i}\right)+\text{reaction} \\ V\frac{\mathrm{d}}{\mathrm{d}t}C_\mathrm{p} &= \left(\sum_{n\text{tissues}}\frac{FC_i}{R_i}\right)-\frac{FC_\mathrm{p}}{R_\mathrm{p}} \end{aligned} \tag{4}$$

where C, V, have usual meanings, R is the partition coefficient, I the chamber/tissue type, p the plasma compartment and, R_p the refers to plasma protein binding. The accurate application of these equations to the μCCA requires some modification however. V refers to tissue volume, with the assumption that "tissue" implies the typical cell, interstitial space, and blood amounts found in living tissue. The μCCA has a different composition, and hence needs to be treated accordingly. To accommodate this, we replace C and V in the above equations with the tissue intracellular C_cell and V_cell, and the tissue extracellular C_ext and V_ext. By using chain differentiation and substituting $R = C_\mathrm{Cell}/C_\mathrm{Liquid}$, then rearranging we obtain a modified equation that can be used for either in vivo tissues or our μCCA chambers:

$$\frac{\mathrm{d}}{\mathrm{d}t}C_\mathrm{Cell} = F \times \frac{(C_\mathrm{plasma}/R_\mathrm{Plasma}-C_\mathrm{Cell}/R_\mathrm{Cell})+\text{reaction}}{V_\mathrm{Liquid}/R_\mathrm{Cell}+V_\mathrm{Cell}} \tag{5}$$

The flow structure used for the human and μCCA PBPK simulations are illustrated in Figure 3. Although these two structures differ, when each is simulated with the same animal parameters for the corresponding tissues, the dynamics are similar (Tatosian, 2007). Data for partitioning in the CCA obtained from in vitro incubations, and for human obtained from the literature (Harris and Gross, 1975) are presented in Table I. The reaction terms in this case are estimated by the results of the C3A metabolism experiments.

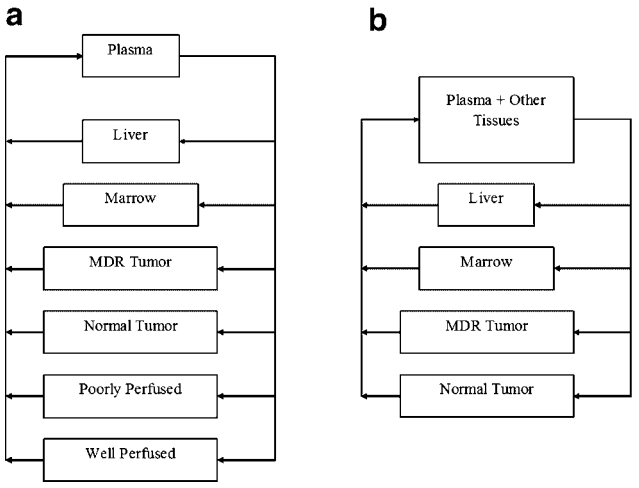

Figure 3. Comparison of (**a**) human simplified PBPK, and (**b**) the μCCA layout. In the μCCA, the Plasma + Other tissues volume is contained within the debubbler.

Results

We have designed and fabricated a μCCA device to evaluate drug-dosing strategies to treat MDR and normal cancer, and then compare the response to individual cell lines in traditional 96-well plate assays. The μCCA contains four cell lines located in different chambers: HEP/G2-C3A (C3A), from a hepatoma; MEG-01 (MEG01), a megakaryoblast; MES-SA (MESSA), a uterine sarcoma; and MES-SA/DX-5 (DX5), a sub-line selected for resistance to doxorubicin (Harker and Sikic, 1985). These two cell lines (MESSA and DX5) are presumably identical except for expression of the MDR phenotype due to P-gp over expression (Park and James, 2003). While the C3A cell line is derived from a hepatoma it has been selected for a relatively high level expression of various cytochrome P450 isozymes and its relative "normal" behavior such as contact inhibition. The MEG-01 cell line represents a cell function that is sensitive to some chemotherapies and, thereby, becomes dose limiting.

Using the μCCA device, we have performed several studies with the model drug doxorubicin (DOX) and the drug modulators nicardipine (NCP) and cyclosporine A (CSP). DOX is an anthracycline drug commonly used to treat both solid tumors and leukemia, and is metabolized into a less active but toxic metabolite doxorubicinol (DOXOL); the impact of metabolism is captured by the inclusion of the hepatocyte cell line. DOX has known toxicity to bone marrow blood progenitors, including depletion of platelet and platelet producing cells (thrombocytopenia); this fact indicated the use of the MEG-01 cell line as an indicator of systemic toxicity. NCP is a calcium channel blocker, and CSP is an immunosuppressant; both are well-documented MDR modulators (Krishna and Mayer, 2000).

Acute Cytotoxicity

The first experiment was to evaluate the cytotoxic response due to DOX and modulator exposure during a 24 h period of time. Based on a preliminary dose-exploration experiment (Supplementary Fig. 2), 10 μM DOX was selected as the base chemotherapeutic concentration for acute cytotoxicity experiments in the device. When the μCCA is dosed with 10 μM DOX, the four cell types exhibit varied viability responses (Fig. 4b), with the sensitive tumor cell line MESSA near 50% cell death, and the resistant cell type DX5

Table I. List of partition values used for the PBPK models.

	Liver	Marrow	Uterus (MDR)	Uterus (muscle)	Plasma	Well perfused (lungs)	Poorly perfused (fat)
Human (rabbit)	45	91	17.2	29	2.8	57	19
μCCA	66.5	144.6	45.3	76.4	0.23	—	—

Human data were obtained from a rabbit model (Harris and Gross, 1975), with the exception of the MDR tissue, which was scaled by the ratio of DX5 to MESSA partition values (since no other in vivo data were available for this tissue). μCCA partition coefficients for DOX were determined experimentally for the C3A, MEG01, MESSA, and DX5 cell lines.

displaying negligible response; the C3A (''liver'') cell line shows a significant decrease in viability to 71% from 100%. Both MDR modulators, NCP (20 μM) and CSP (10 μM), increased the toxic response in the DX5 cell type dramatically (reducing viability from about 91% to 51%). The presence of NCP (20 μM) and CSP (10 μM) had little additional effect (not exceeding 10% reduction) from DOX alone on the MESSA, C3A, and MEG01 cell lines. When NCP and CSP are mixed at 5 μM each for a total MDR modulator concentration of 10 μM, toxicity is further enhanced in the DX5 cell line (50–28% viability), modestly enhanced in C3A (~64–45%), and not altered in the MESSA and MEG01 cell lines.

The MEG01 cell type in the device typically exhibits a baseline viability of ~80%, as reported by the assay used, in contrast to the near 100% baseline viability of the other cell types. This is due to the presence of small cell particles in these cell chambers. This cell type is known to produce platelet-like particles, which have reduced metabolic activity compared to normal platelets (Takeuchi et al., 1991, 1995, 1998). The formation of these particles occurs in healthy and functional MEG01 cells, and shear stress is believed to aid in releasing them from the cell body (Takeuchi et al., 1998). These platelet-like particles can usually be filtered out during analysis due to their small size, but larger particles or aggregates are difficult to distinguish from dead cells or cell debris and hence influence the measured viability results (Tatosian, 2007). Therefore 80% viability as determined by this assay for this cell type on the chip is considered normal.

Relative Doxorubicin Uptake

In addition to assessing viability in the device, we also assessed drug pharmacokinetics in the μCCA by measuring the relative drug uptake into each cell type using fluorescence microscopy. After a 24 h exposure in the μCCA device the uptake of doxorubicin was enhanced by addition of either modulator (Fig. 5). Additionally, a comparison of the magnitude of drug uptake with the corresponding viability shows a general relationship between uptake and toxicity. For example, in our results for DX5 viability, combining DOX with either CSP or NCP resulted in increasing toxicity in the μCCA compared to DOX alone (Fig. 4). Similarly, DOX fluorescence in the DX5 cells increased when combined with either modulator.

Cell Response in 96 Well Plates

To compare the results from the μCCA to typical in vitro results, a 96-well plate assay was used. Five test mixtures containing serial dilutions of DOX (range: 0.025–25 μM) combined with CSP or NCP (DOX alone, DOX plus 5 μM CSP, DOX plus 5 μM NCP, DOX plus 5 μM CSP and 5 μM NCP, and DOX plus 2.5 μM CSP and 2.5 μM NCP) were used to find the DOX concentration resulting in a 50% reduction in viability/proliferation or EC_{50} value. Similarly the EC_{30} value was found for 30% viability reduction. Due to technical difficulties at higher concentrations, probably due to the release of platelet-like particles that aggregated, an EC_{50} value could not be determined accurately for the

Table II. Values of EC50 and EC30 for individual cell types in static culture.

	EC_{50} (μM)				EC_{30} (μM)			
Test solution	C3A	DX5	MESSA	MEG01	C3A	DX5	MESSA	MEG01
(a) 10 μM DOX	3.1	270[a]	0.96	[b]	1.3	13	0.50	4.9
(b) +5 μM CSP	0.40	0.46	0.53	[b]	0.22	0.20	0.24	0.22
(c) +5 μM NCP	1.2	6.4	1.0	[b]	0.75	1.0	0.58	0.79
(d) +5 μM CSP/NCP	0.25	0.29	0.50	[b]	0.12	0.09	0.24	0.15
(e) +2.5 μM CSP/NCP	0.36	1.6	0.70	[b]	0.20	0.61	0.32	0.38

Using a 96-well plate format and a MTS assay for viability, dose–response curves were determined for each cell type using serial dilutions of DOX (range: 0.025–25 μM) combined NCP or CSP in the following 5 test solutions: (a) DOX alone, (b) DOX with 5 μM CSP, (c) DOX with 5 μM NCP, (d) DOX with 5 μM CSP and 5 μM NCP, and (e) DOX with 2.5 μM CSP and 2.5 μM NCP.

[a]This value is extrapolated beyond the tested conditions, and is qualitative only.

[b]These cells (MEG01) enter apoptosis to form platelet-like cell particles at higher drug exposures and the response is difficult to read due to aggregation of these platelet-like particles, consequently only the lower toxicity (EC_{30}) values are reported.

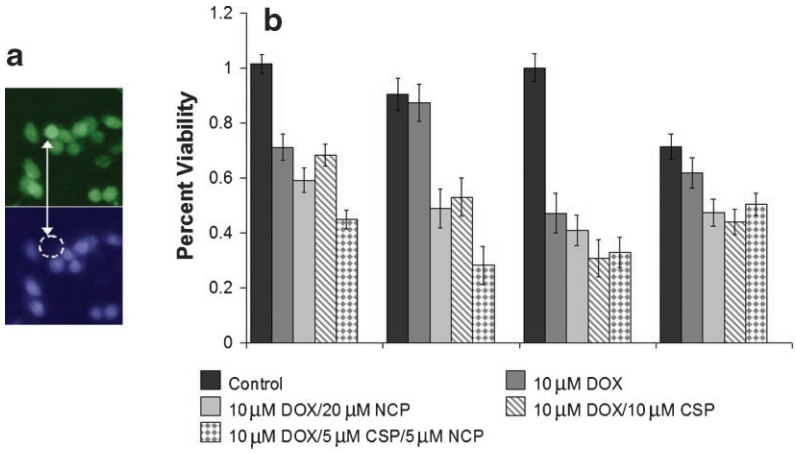

Figure 4. Results of acute toxicity study with the μCCA device. **a**: Illustration of assay used to determine viability. Green cells (top) labeled with CellTracker Green, blue cells (bottom) labeled with Calcein Blue. Cells that are visible in the green image but missing in the blue image have begun cell death (an example is indicated with the arrow). **b**: Resulting percent viability in each cell type in response to drug mixture exposure. Note the significant decrease in viability in the DX5 cell line when the mixture of modulators is used. Error bars = 1 standard deviation, *n* μCCA samples > 40 for each cell type.

MEG01 cells, but an EC_{30} value could be obtained. Results are shown in Table II.

The MDR modulators had a significant effect on the DOX EC_{50} and EC_{30} values for all cell lines. This result is unlike that in the μCCA where the MDR modulators had little additional impact on viability in the MESSA and MEG01 cell lines. Also DOX with CSP was more potent than DOX with NCP. When the total dose of MDR suppressor was maintained at 5 μM by using 2.5 μM NCP and 2.5 μM CSP, the DOX EC_{50} value was intermediate between treatment with 5 μM CSP or 5 μM NCP alone. This response suggests an additive rather than synergistic response to these drug mixtures (except for C3A where the 2.5 μM mixture shows slightly enhanced toxicity). These responses are in clear contrast to the μCCA experiments where a strong, cell-specific synergistic response was observed in the DX5 cell line, but not the other cell lines.

Two primary differences between the 96-well plate assay and the μCCA flow experiment is the exchange of metabolites between compartments and the effect of fluid flow on cell physiology. Consequently we designed a test of the effect of flow on cell proliferation.

μCCA Versus Static: Comparison of Growth Rates

Shear stress is known to influence cell growth and activity of cultured mammalian cells (Essig and Friedlander, 2003; Kan

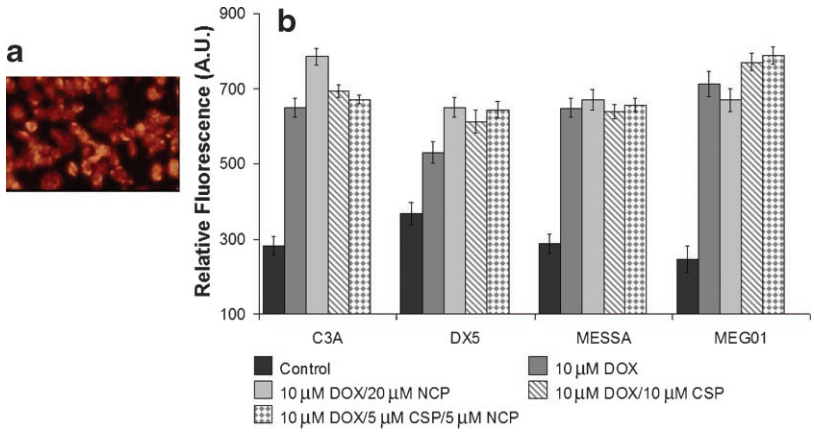

Figure 5. **a**: Fluorescent image of doxorubicin taken up by the cells in the device. **b**: Relative fluorescence of doxorubicin in each cell type following exposure, showing corresponding drug levels to the viability results in Figure 4. Note the significant difference in accumulation in the drug resistant cell line DX5 upon addition of any of the drug modulators. This corresponds reasonably well with the reduction in viability seen in Figure 4. Error bars = 1 standard deviation, *n* μCCA samples > 40 for each cell type.

Table III. Ratio of cell growth in recirculation versus static μCCA culture.

	C3A	DX5	MESSA	MEG01
Ratio (flow/static)	0.40	0.71	0.62	0.59
Standard error	0.03	0.05	0.04	0.05

$n \geq 10$ for each condition.

et al., 2004). To investigate the impact of shear on growth rate, we compared cell growth rate on control μCCA chips in static culture dishes containing 10 mL culture medium to the growth rate of cells in the recirculating μCCA device. The medium per chip in the culture wells was 2.5 mL, compared to 250 μL per chip in the recirculating devices. The reduction in growth rate of cells in the μCCA system is presented in Table III. All cell types had reduced growth in the recirculating μCCA system, though the C3A cells were most affected. We can only speculate on the reasons for those differences (see Fig. 6), but the effects of hydrodynamic shear, reduction in nutrient availability, exchange of metabolites or accumulation of cell waste material like ammonia are probable factors.

Selective Synergistic Drug Effects on Cell Proliferation

In contrast to short-term experiments where high drug concentrations were used, we also performed 3-day proliferation experiments using more physiologically realistic concentrations of drugs. The purpose of this experiment is to compare the reduction in growth/tissue shrinkage after exposure to the chemotherapeutic and modulator cocktails. Total cell density was assayed by fluorescent imaging and cell counting using the probe, CellTracker Green.

Results comparing the impact of DOX and the modulators on cell proliferation are summarized in Figure 7. The "control" data shown refer to control medium without drugs recirculated through the device (i.e., flow control). All cell types show some reduction in proliferation when exposed to the chemotherapy drug, with the drug sensitive (MES-SA) cells exhibiting the most significant drop in growth due to DOX (2.5-fold). The impact of modulators is similar to that observed in the acute toxicity study, with clear synergy between CSP and NCP in modulating effectiveness selectively against the MDR resistant DX5 cell line. The combination of 1 μM DOX, 5 μM CSP, and 5 μM NCP resulted in more than a fivefold decrease in proliferation of MES-SA/DX-5 cells. Indeed, this was the only compartment to show a net decrease in cells. The mixture of NCP and CSP has no statistically significant difference on proliferation in the other cell types when compared to 1 μM DOX alone (P-values: C3A = 1.0, MESSA = 0.26, MEG01 = 0.96).

Dosage Comparison—μCCA Versus Human

In many in vitro diagnostic screens, relating the selected drug concentrations to a therapeutic clinical dose is often difficult. Typical doses of DOX are in the 50–110 mg/m^2 range, with higher doses often requiring recovery steps such as stem cell replacement (Honkoop et al., 1997). To compare the exposure resulting from these doses with the doses used

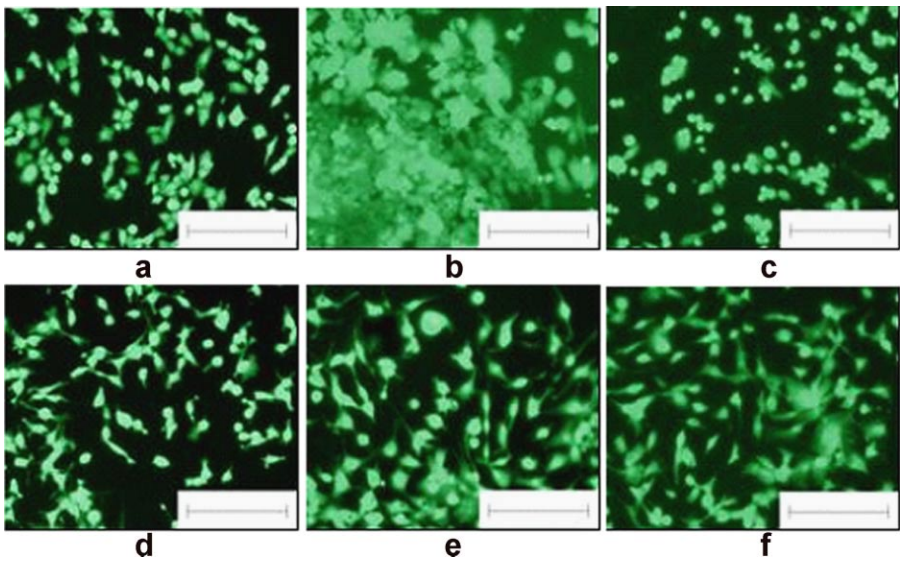

Figure 6. Representative images of MESSA cells (**a**–**c**) and C3A cells (**d**–**f**) taken from an initial time point (a, d), 72 h exposure to control medium (b,e), and 72 h exposure to 1 μM DOX–10 μM NCP (c,f). Cells are labeled with CellTracker Green, and the scalebar = 200 μm. From the images in Figure 2c and f, the MESSA cells (c) and C3A cells (f) cultured for 3 days in the μCCA device display morphology similar to cells growing in normal culture flasks, which may suggest that stress was not a significant issue. In contrast, the MESSA cells (Fig. 2d) displayed noticeable changes in cell morphology when exposed to 1 μM DOX for 3 days, while the C3A cells (Fig. 2f) maintained a relatively normal morphology, further illustrating that this dose condition is less stressful to C3A then to MESSA. [Color figure can be seen in the online version of this article, available at www.interscience.wiley.com.]

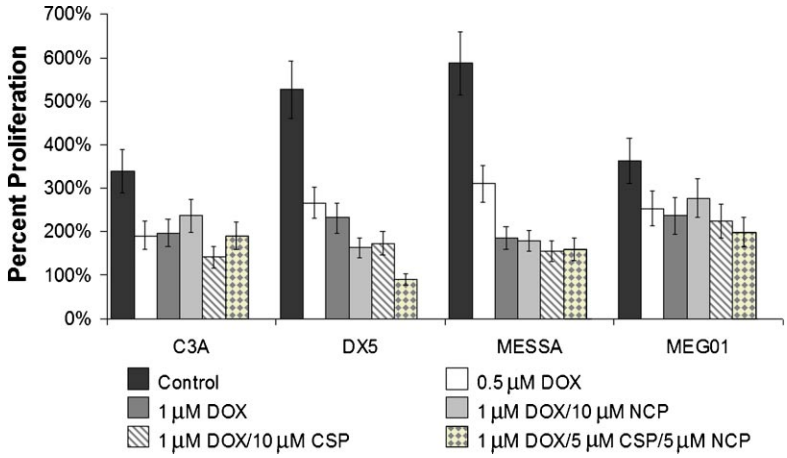

Figure 7. Three days proliferation reduction study on μCCA. Relative proliferation of each cell type in the μCCA device during 72 h exposure. Growth is expressed as percentage of growth compared to the initial amount of cells on the device before beginning drug exposure. Error bars = 1 standard deviation, *n* μCCA samples > 40 for each cell type. [Color figure can be seen in the online version of this article, available at www.interscience.wiley.com.]

in our μCCA experiments, we have built a PBPK model for both humans and the μCCA device to simulate the distribution of DOX and the major metabolite doxorubicinol (DOXOL).

We have compared the distribution profiles of DOX and DOXOL in the different tissues resulting from 72 h exposure to 100 mg/m^2 dose of DOX in human plasma and 1 μM DOX in the μCCA culture medium (Fig. 8). The plasma area

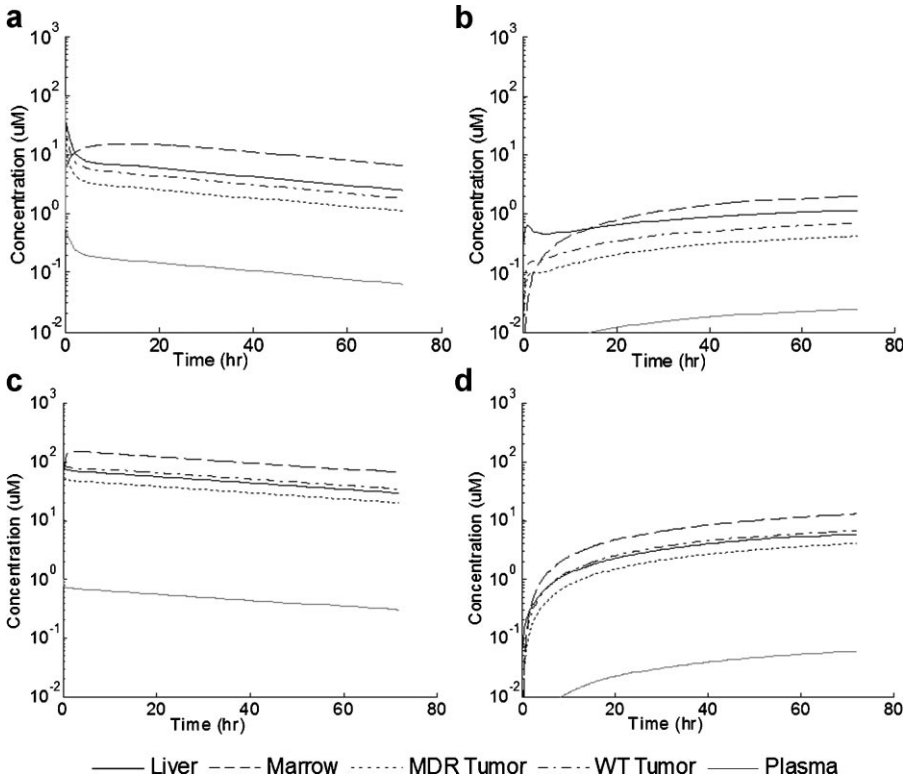

Figure 8. Comparison of PBPK Simulations in Human at 100 mg/m^2 of DOX exposure and μCCA at 1 μM DOX. Each graph shows predicted pharmacokinetic profiles of doxorubicin and its major metabolite doxorubicinol in a human organ model, and in the μCCA compartments. **a**: DOX and (**b**) DOXOL predicted in humans; (c) DOX and (d) DOXOL simulated in the μCCA device.

under the curve (AUC) predictions for the human PBPK (DOX: 1.1 mM min, DOXOL: 0.11 mM min) is less than the μCCA (DOX: 3.4 mM min, DOXOL: 0.25 mM min), though they are on the same order of magnitude.

The primary reason for the larger AUC and distribution profiles in the μCCA compared to the human model is the large holdup volume associated with the external debubbler/reservoir/sample port representing the hold up in other tissues, plasma, and compartments. Additionally, the partition coefficients used in the PBPK models are different. The human coefficients are based on the normal tissue microenvironment, while the μCCA partition coefficients are obtained from cell monolayer cultures; hence the values are not identical.

An additional design constraint is the liquid to cell ratio attainable in our experimental system. The target volume ratio found in vivo is approximately 2:1 cell to liquid, while the closest practically obtainable value in our fabricated devices with cell monolayers and a debubbler/reservoir is approximately 1:5. As a point of contrast, typical culture vessels such as 96 well plates have a ratio of on the order of 1:50. By implementing these mathematical models, we can plan our doses to accommodate these design challenges and still mimic clinically realistic exposures.

Discussion

The described method illustrates a novel in vitro experimental system to predict efficacy of chemotherapeutic/modulator mixtures to kill MDR tumor cells or to reduce their growth selectively in vivo with tolerable side effects on normal tissues. Currently available methods rely on the use of isolated populations of target human cells in vitro to predict human efficacy, and animal models to predict drug safety. Pharmacokinetic interactions are not identified until animal trials begin, and frequently require clinical trials to detect. Indeed the synergy of the two MDR suppressors is observed in the μCCA but not in traditional well plate assays. The μCCA approach is well suited to studying pharmacokinetic interactions between cell types and the resulting cellular response. Incorporating PBPK predictions of in vivo dose levels can allow matching of drug exposure between the μCCA device and animal or human trials. The system also requires very small amounts of material to perform studies, which is beneficial in early screening of novel compounds. Another application of the μCCA device is hypothesis testing for toxic and metabolic interactions. Different tissues may be modeled with the device to investigate other potential interactions, and to discover dose limiting cell types. Additionally, ''Knockout Devices'' may easily be made by excluding a cell type in some experiments, to isolate effects of that cell on others in the system.

These proof-of-concept experiments demonstrate the potential of the μCCA approach to testing chemical and drug mixtures in general. In both drug testing and environmental toxicity testing, evaluation of mixtures remains particularly challenging. Unlike other in vitro systems this approach allows evaluation of the whole system, not an isolated component. Further it facilitates conversion of experimental results to relevant predictions of human response.

Particularly important is the observation of cell selective synergy of the two MDR modulators tested (see Figs. 4 and 7). While it would be expected that the MDR modulators would affect the DX5 cell line preferentially, due to its over-expression of P-gp, the synergistic interaction of NCP and CSP is unexpected. Such a synergistic response in DX5 in a static assay system is not observed. The particular mechanism is unknown, but exchange of metabolites and response to flow are two key differences. Such synergy may be important practically. The use of MDR suppressors in clinical trials has been unsuccessful due to side effects. Use of multiple MDR suppressors with each at a reduced dose and having different side effects may be better tolerated by patients than a single modulator at a higher dose (Lehnert et al., 1991; Pascaud et al., 1998).

The μCCA system has the potential to be multiplexed to allow a large number of simultaneous experiments. In other studies (Oh et al., 2007; Tatosian et al., 2005) we are developing detection systems that will allow the near real time integration of many units. We believe that multiple chips can be mounted in arrays of 96 units to facilitate more rapid evaluation of multiple dosing strategies. We are also working on the use of tissue-engineered constructs instead of monolayer cultures. Such constructs should allow us to construct more biochemically and physiologically accurate models. Such in vitro models offer the possibility of reducing our dependence on animal models while making more relevant human predictions as such devices can readily use human cells.

This research was sponsored, in part, by the New York State Office of Science, Technology and Academic Research (NYSTAR) program, the National Science Foundation (BES 0342985). This material is based upon work supported in part by the STC Program of the National Science Foundation under Agreement No. ECS-9876771. This work was performed in part at the Cornell Nano-Scale Science & Technology Facility (a member of the National Nanofabrication Users Network) which is supported by the National Science Foundation under Grant ECS-9731293, its users, Cornell University and Industrial Affiliates.

References

Anderson AB, Gergen J, Arriaga EA. 2002. Detection of doxorubicin and metabolites in cell extracts and in single cells by capillary electrophoresis with laser-induced fluorescence detection. J Chromatogr B Anal Technol Biomed Life Sci 769(1):97–106.

Borowski E, Bontemps-Gracz MM, Piwkowska A. 2005. Strategies for overcoming ABC-transporters-mediated multidrug resistance (MDR) of tumor cells. Acta Biochim Pol 52(3):609–627.

Dessypris EN, Brenner DE, Hande KR. 1986. Toxicity of doxorubicin metabolites to human marrow erythroid and myeloid progenitors in vitro. Cancer Treat Rep 70(4):487–490.

D'Souza RW, Boxenbaum H. 1988. Physiological pharmacokinetic models: Some aspects of theory, practice and potential. Toxicol Ind Health 4(2):151–171.

Essig M, Friedlander G. 2003. Tubular shear stress and phenotype of renal proximal tubular cells. J Am Soc Nephrol 14 (Suppl 1): S33–S35.
Gerlowski LE, Jain RK. 1983. Physiologically based pharmacokinetic modeling: Principles and applications. J Pharm Sci 72(10):1103–1127.
Ghanem A, Shuler ML. 2000. Combining cell culture analogue reactor designs and PBPK models to probe mechanisms of naphthalene toxicity. Biotechnol Prog 16(3):334–345.
Gigli M, Doglia SM, Millot JM, Valentini L, Manfait M. 1988. Quantitative study of doxorubicin in living cell nuclei by microspectrofluorometry. Biochim Biophys Acta 950(1):13–20.
Harker WG, Sikic BI. 1985. Multidrug (pleiotropic) resistance in doxorubicin-selected variants of the human sarcoma cell line MES-SA. Cancer Res 45(9):4091–4096.
Harris PA, Gross JF. 1975. Preliminary pharmacokinetic model for adriamycin (NSC-123127). Cancer Chemother Rep 59(4):819–825.
Honkoop AH, van der Wall E, Feller N, Schuurhuis GJ, van der Vijgh WJF, Boven E, van Groeningen CJ, Giaccone G, Hoekman K, Vermorken JB, Wagstaff J, Pinedo HM. 1997. Multiple cycles of high-dose doxorubicin and cyclophosphamide with G-CSF mobilized peripheral blood progenitor cell support in patients with metastatic breast cancer. Ann Oncol 8(10):957–962.
Hooiveld GJEJ, Heegsma J, van Montfoort JE, Jansen PLM, Meijer DKF, Muller M. 2002. Stereoselective transport of hydrophilic quaternary drugs by human MDR1 and rat Mdr1b P-glycoproteins. Br J Pharmacol 135(7):1685–1694.
Johnstone RW, Cretney E, Smyth MJ. 1999. P-glycoprotein protects leukemia cells against caspase-dependent, but not caspase-independent, cell death. Blood 93(3):1075–1085.
Kan P, Miyoshi H, Ohshima N. 2004. Perfusion of medium with supplemented growth factors changes metabolic activities and cell morphology of hepatocyte-nonparenchymal cell coculture. Tissue Eng 10(9–10):1297–1307.
Karukstis KK, Thompson EHZ, Whiles JA, Rosenfeld RJ. 1998. Deciphering the fluorescence signature of daunomycin and doxorubicin. Biophys Chem 73(3):249–263.
Kirchmeier M, Ishida T, Chevrette J, Allen T. 2001. Correlations between the rate of intracellular release of endocytosed liposomal doxorubicin and cytotoxicity as determined by a new assay. J Liposome Res 11(1): 15–29.
Krishna R, Mayer LD. 2000. Multidrug resistance (MDR) in cancer. Mechanisms, reversal using modulators of MDR and the role of MDR modulators in influencing the pharmacokinetics of anticancer drugs. Eur J Pharm Sci 11(4):265–283.
Lehnert M, Dalton WS, Roe D, Emerson S, Salmon SE. 1991. Synergistic inhibition by verapamil and quinine of P-glycoprotein-mediated multidrug resistance in a human myeloma cell line model. Blood 77(2):348–354.
Maniez-Devos DM, Baurain R, Trouet A, Lesne M. 1985. Doxorubicin pharmacokinetics in the rabbit. J Pharmacol 16(2):159–169.
Oh TI, Sung JH, Tatosian DA, Shuler ML, Kim D. 2007. Real-time fluorescence detection of multiple microscale cell culture analog devices in situ. Cytometry A 71(10):857–865.
Olson RD, Mushlin PS, Brenner DE, Fleischer S, Cusack BJ, Chang BK, Boucek RJ. 1988. Doxorubicin cardiotoxicity may be caused by its metabolite, doxorubicinol. Proc Natl Acad Sci USA 85(10):3585–3589.
Park S, James CD. 2003. Lanthionine synthetase components C-like 2 increases cellular sensitivity to adriamycin by decreasing the expression of P-Glycoprotein through a transcription-mediated mechanism. Cancer Res 63(3):723–727.
Pascaud C, Garrigos M, Orlowski S. 1998. Multidrug resistance transporter P-glycoprotein has distinct but interacting binding sites for cytotoxic drugs and reversing agents. Biochem J 333 (Pt 2): 351–358.
Shuler ML, Ghanem A, Quick D, Wong MC, Miller P. 1996. A self-regulating cell culture analog device to mimic animal and human toxicological responses. Biotechnol Bioeng 52(1):45–60.
Sin A, Chin KC, Jamil MF, Kostov Y, Rao G, Shuler ML. 2004. The design and fabrication of three-chamber microscale cell culture analog devices with integrated dissolved oxygen sensors. Biotechnol Prog 20(1):338–345.
Sweeney LM, Shuler ML, Babish JG, Ghanem A. 1995. A cell culture analogue of rodent physiology: Application to naphthalene toxicology. Toxicol In Vitro 9(3):307–316.
Takeuchi K, Ogura M, Saito H, Satoh M, Takeuchi M. 1991. Production of platelet-like particles by a human megakaryoblastic leukemia cell line (MEG-01). Exp Cell Res 193(1):223–226.
Takeuchi M, Kuno H, Satoh M, Yoshida T, Ogura MTK. 1995. Platelet-like particles released by inhibition of DNA synthesis in the human megakaryoblastic leukemia cell line, MEG-01s. Tissue Cult Res Commun 14:165–175.
Takeuchi K, Satoh M, Kuno H, Yoshida T, Kondo H, Takeuchi M. 1998. Platelet-like particle formation in the human megakaryoblastic leukaemia cell lines, MEG-01 and MEG-01s. Br J Haematol 100(2):436–444.
Tatosian DA. 2007. Development of a microscale cell culture analog device to study multidrug resistance modulators [Doctoral]. Ithaca: Cornell University. p. 186.
Tatosian DA, Shuler ML, Kim D. 2005. Portable *in situ* fluorescence cytometry of microscale cell-based assays. Opt Lett 30(13):1689–1691.
Tsuruo T, Naito M, Tomida A, Fujita N, Mashima T, Sakamoto H, Haga N. 2003. Molecular targeting therapy of cancer: Drug resistance, apoptosis and survival signal. Cancer Sci 94(1):15–21.
Viravaidya K, Shuler ML. 2004. Incorporation of 3T3-L1 cells to mimic bioaccumulation in a microscale cell culture analog device for toxicity studies. Biotechnol Prog 20(2):590–597.
Viravaidya K, Sin A, Shuler ML. 2004. Development of a microscale cell culture analog to probe naphthalene toxicity. Biotechnol Prog 20(1): 316–323.
Wong JK, Kennedy PR, Belcher SM. 2001. Simplified serum- and steroid-free culture conditions for high-throughput viability analysis of primary cultures of cerebellar granule neurons. J Neurosci Methods 110(1–2):45–55.
Zhou Q, Chowbay B. 2002. Determination of doxorubicin and its metabolites in rat serum and bile by LC: Application to preclinical pharmacokinetic studies. J Pharm Biomed Anal 30(4):1063–1074.